Anatomical relationships between medullary veins and three types of deep-seated malignant brain tumors as detected by susceptibility-weighted imaging

Shih-Hung Yang[a,b], Chien-Tai Hong[c,d], Fong Y. Tsai[e,f], Wei-Yu Chen[g], Chia-Yuen Chen[a,b,*], Wing P. Chan[a,b]

[a]Department of Radiology, Wan Fang Hospital, Taipei Medical University, Taipei, Taiwan, ROC; [b]Department of Radiology, School of Medicine, College of Medicine, Taipei Medical University, Taipei, Taiwan, ROC; [c]Department of Neurology, Shuang Ho Hospital, Taipei Medical University, New Taipei City, Taiwan, ROC; [d]Department of Neurology, School of Medicine, College of Medicine, Taipei Medical University, Taipei, Taiwan, ROC; [e]Department of Radiological Sciences, University of California Irvine, Irvine California, USA; [f]Imaging Research Center, Taipei Medical University, Taipei, Taiwan, ROC; [g]Department of Pathology, Wan Fang Hospital, Taipei Medical University, Taipei, Taiwan, ROC

Abstract

Background: Deep-seated brain tumors can be difficult to differentiate. Three tumor types (primary central nervous system lymphoma [PCNSL], high-grade glioma, and metastatic brain tumors), identified by susceptibility-weighted imaging, have different relationships with small medullary veins, and these relationships can be used to enhance diagnostic accuracy.

Methods: Records of patients with pathology confirmed malignant brain tumors who received susceptibility-weighted imaging between 2009 and 2015 were reviewed. A total of 29 patients with deep-seated malignant brain tumors in the territory of small medullary veins were enrolled in this study. The sensitivity, specificity, and diagnostic accuracy of medullary vein blockage (MVB), defined as a small medullary vein terminating at the margin of the tumor, for indicating malignant brain tumors were analyzed.

Results: Of 11 patients with PCNSLs, 5 with high-grade gliomas, and 13 with metastases, only the latter presented MVBs. The sensitivity, specificity, and accuracy of using MVBs for diagnosing metastatic tumors were 76.9%, 100%, and 89.7%, respectively.

Conclusion: An MVB is an accurate sign for differentiating metastatic brain tumors from two other common malignancies and thus provides a useful tool for preoperative planning.

Keywords: Brain; Magnetic resonance imaging; Medullary vein; Metastasis; Susceptibility-weighted imaging

1. INTRODUCTION

Metastases, high-grade gliomas, and primary central nervous system lymphomas (PCNSLs) are adult brain malignancies commonly encountered in neuroradiologic diagnostic settings. Accurate preoperative diagnoses of these malignancies are crucial so that their distinct managements and prognoses are properly applied.[1–3] The differential diagnosis of the three brain malignancies is challenging because their neuroimaging presentation are highly variable and overlapping with each other. For example, each of them can occur as single or multiple masses, appear as circumscribed or well-enhanced lesions in either cerebral hemisphere, and can be accompanied by necrosis or hemorrhage. This is particularly true when a metastatic tumor is solitary and/or located in the deep structure of the brain rather than exhibiting the more commonly presented multiple and superficial presentation.

These deep-seated malignant tumors are similar in conventional magnetic resonance (MR) imaging sequences such as fluid attenuation inversion recovery imaging and T1-weighted (T1W) contrast enhancement patterns, which reflect only the degree of blood-brain barrier breakdown.[4,5] Advanced MR imaging sequences, including diffusion-weighted images, provide information about apparent diffusion coefficient maps, where low values are observed in brain tumors because of their high cellular density,[6] a common factor in all three of these tumor types. The metabolic information revealed by MR spectroscopy benefits diagnosis. However, variations in study quality, patient population, and study design have caused heterogeneity between individual studies, limiting the application.[7]

Susceptibility-weighted imaging (SWI) is a new MR sequence that uses gradient-recalled echo phase images to demonstrate the smallest susceptibility variations in the corresponding magnitude images.[8–10] This sequence has been used to differentiate PCNSLs from high-grade gliomas by the number of susceptibility-based signals or intratumoral susceptibility signals. The

*Address correspondence: Dr. Chia-Yuen Chen, Department of Radiology, Wan Fang Hospital, Taipei Medical University, 111, Section 3, Hsing-Long Road, Taipei 116, Taiwan, ROC. E-mail address: chiayuenchen@gmail.com (C.-Y. Chen).

Author Contributions: Dr. Shih-Hung Yang and Dr. Chien-Tai Hong contributed equally to this article.

Conflicts of Interest: The authors declare that they have no conflicts of interest related to the subject matter or materials discussed in this article.

Journal of Chinese Medical Association. (2020) 83: 164-169.

Received May 2, 2018; accepted November 8, 2019.

doi: 10.1097/JCMA.0000000000000235.

presence of intratumoral susceptibility signals can be used to differentiate between glioblastomas and PCNSLs with high sensitivity (91.2%) and specificity (93.3%).[11,12] Also, SWI is highly sensitive for detecting intravascular venous deoxygenated blood even when the venous vasculature is smaller than one voxel because paramagnetic deoxyhemoglobin is used as an intrinsic contrast agent.[13,14] Therefore, small medullary veins in deep brain structures can easily be detected, an outcome that has not been achieved with conventional MR imaging. Since these small medullary veins are distal part of the deep venous system,[15] their territory will be used to define whether a tumor is deep-seated and to observe the anatomical relationships between tumors and adjacent small medullary veins in this study.

Histologically, these three malignant tumor types have distinct growth patterns that can affect how each is associated with medullary veins. High-grade glioma is infiltrative, and PCNSL is characterized by a cluster of malignant lymphocytic cells surrounding the pre-existing vessels.[1] Vessels can be entrapped within either of these two tumor types. In contrast, a metastatic brain tumor has a well-defined border and pushes brain parenchyma and adjacent pre-existing vessels away.[1,16–21] Based on this differing characteristic, we hypothesized that the anatomical relationships between tumors and adjacent small medullary veins would differ in these three common types of malignant brain tumors, and that SWI, which is adept at detecting small medullary veins, could provide crucial information that would allow differentiation.

2. METHODS

2.1. Patients

This study was approved by the Joint Institutional Review Board of Taipei Medical University (approval no. N201603081). Informed consent was waived because the study was a retrospective review.

The database maintained by the Pathology Department at our institution showed that 72 patients had pathologically confirmed PCNSLs, high-grade gliomas, or metastatic brain tumors between May 2009 and March 2015. Records were reviewed, and patients were excluded if motion artifacts were marked or if only postoperation or postbiopsy SWI images were available. Patients were included if complete MR images, including SWI sequences, were available and if their tumors were deep-seated in the territory of small medullary veins, which was defined as the epicenter of at least one tumor located medial to the ipsilateral imaginary line drawn connecting the endpoints of each medullary veins of one side (Fig. 1; see Fig. 2C for the example of a deep-seated tumor).

Based on the above-mentioned criteria, a total of 54 patients, including 11 PCNSLs, 9 high-grade gliomas, and 34 metastases, were recruited for analysis. Among these cases, there were 11 PCNSLs, 5 high-grade gliomas, and 13 metastases in the medullary vein territory. Seven metastases in the cerebellum were not enrolled.

2.2. MR imaging protocol

All MR imaging studies were performed at our institution using a 1.5-T scanner (Magnetom Avanto; Siemens Medical Solutions, Erlangen, Germany) with a standard 12-channel head coil. After the routine T1W and T2-weighted fluid attenuation inversion recovery sequence, SWI and contrast-enhanced T1 sequences were performed. To assess the morphology and margin of the brain tumor, contrast-enhanced T1 was performed with a TR/TE of 552/17 ms, a flip angle of 90°, a field of view of 23 cm, a matrix of 224 × 256, and a slice thickness of 5 mm.

For the transverse three-dimensional SWI sequences, the settings were as follows: TR/TE, 49/40 ms; flip angle, 15°; slice thickness, 2 mm with 60 sections per slab; matrix, 224 × 256; 64 slices; and acceleration factor, 2 for the integrated parallel acquisition technique. Minimal intensity projection (minIP) images were reconstructed with an effective minIP thickness of 16 mm. The sequence and all image processing were automated using the Siemens MR scanner platform based on the concepts by Haacke et al.[8] The phase, magnitude, minIP, and SWI images were uploaded and made available on a picture archiving and communication system (IMPAX 6.4; AGFA Healthcare, Mortsel, Belgium). The total scan time for all protocols was less than 30 minutes.

2.3. Image interpretation

All MR images were reviewed together by two neuroradiologists (S.-H.Y.: 6.5 years of neuroradiologic experience and C-Y.C.: 21 years of neuroradiologic experience) who were blinded to

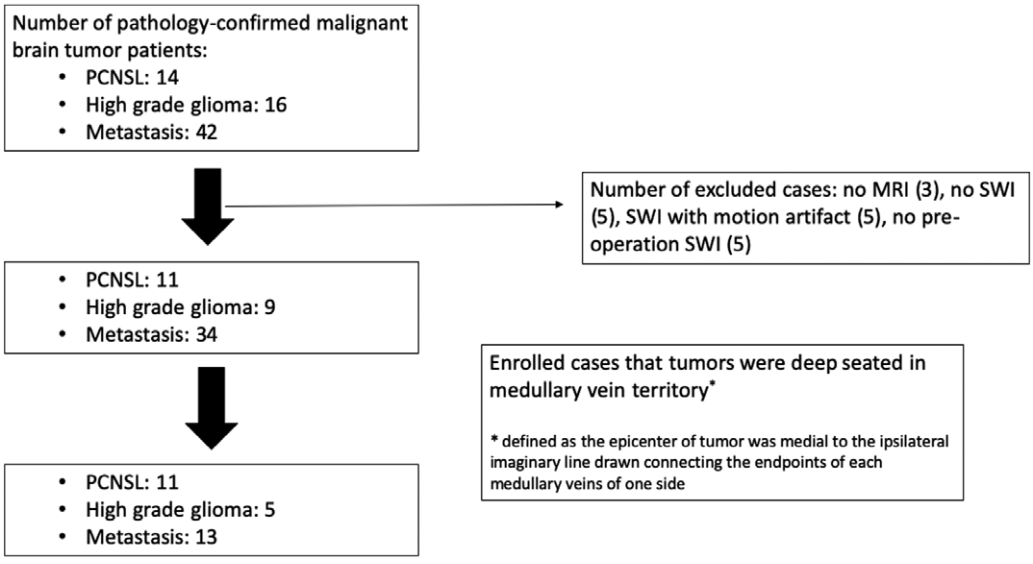

Fig. 1 The selection process used to find patients with malignant brain tumors. MRI = magnetic resonance imaging; PCNSL = primary central nervous system lymphoma; SWI = susceptibility-weighted imaging.

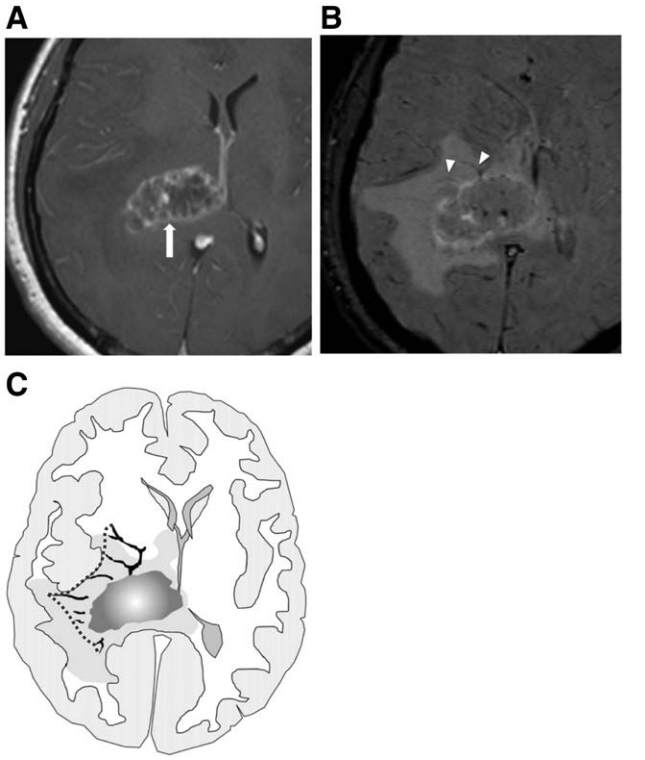

Fig. 2 Representative images of a MVB sign. A 41-year-old woman diagnosed with metastatic adenocarcinoma. A, Axial T1 post-contrast image showing the tumor (arrow) at the right temporoparietal lobe. B, Axial SWI demonstrating the small medullary veins (arrowheads) blocked at the tumoral margin. C, Sketch diagram showing how a contrast-enhanced tumor (A) combined with medullary veins (B), as detected by SWI, a typical example of the MVB sign. The epicenter of the deep-seated tumor is located medial to an imaginary line (dash line) drawn by connecting the endpoints of each medullary veins. MVB, medullary vein blockage; SWI, susceptibility-weighted imaging.

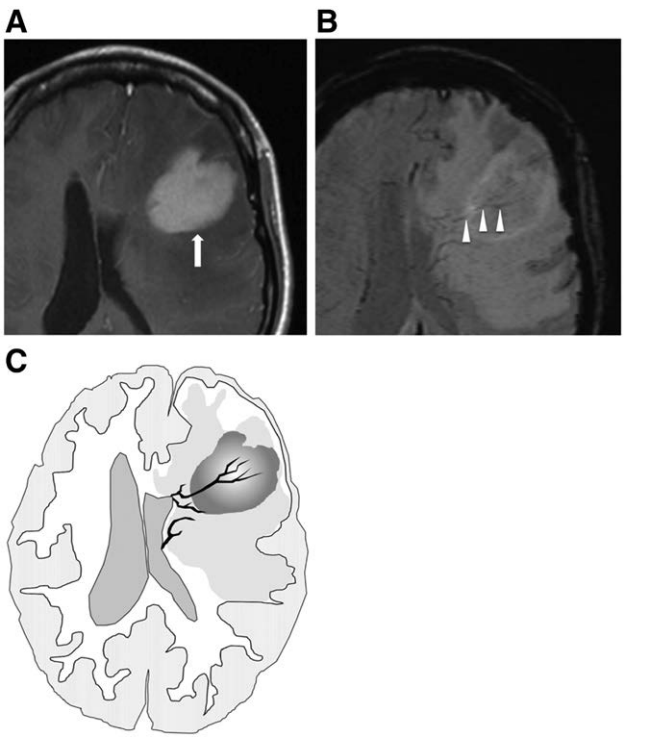

Fig. 3 Representative images of a medullary vein penetrating through the tumor. A 50-year-old woman diagnosed with primary central nervous system lymphoma. A, axial T1 post-contrast image showing the tumor (arrow) at the left frontal lobe. B, axial susceptibility-weighted imaging (SWI) showing a small medullary vein (arrowheads) penetrating through the tumor. C, sketch diagram illustrating the T1 post-contrast image (A) combined with SWI (B) shows the medullary vein passing through the tumor, and it looks like leaf veins.

the pathological diagnoses. Tumoral extent and margin were defined by enhancing a part of the axial contrast-enhanced T1W images. The definition of small medullary veins are veins that merge from the subcortical area, directly cross the white matter, and drained into the subependymal veins.[15] These small medullary veins are not easily identifiable in conventional MR sequences but can be seen in SWI or minIP images as linear and contiguous dark signal intensities perpendicular to the lateral ventricular wall, tapering in the subcortical regions. The anatomical relationships between small medullary veins and tumors in this study were interpreted by correlating contrast-enhanced T1W images with SWI slice by slice until the two neuroradiologists reached consensus for each patient. Different patterns of anatomical relationships were categorized based on the presence of a medullary vein blockage (MVB).

MVB-positive was defined as a small medullary vein terminating at the margin of the tumor (Fig. 2), while MVB-negative was defined when a small medullary vein contiguously penetrated through the tumor along the vessel course without terminating at the margin (Figs. 3 and 4) or the intratumoral SWI signal was unable to be differentiated from blockage or penetration (Fig. 5). When multiple qualified lesions were present and any one exhibited an MVB, the patient was classified as MVB-positive.

2.4. Statistical analysis

The association between the presence of MVB and tumor pathology was analyzed. Descriptive statistics (e.g., mean ± SD or frequency with percentage) were calculated for all variables using IBM SPSS for Windows, Version 19.0 (Released 2010; IBM Corp., Armonk, NY.)

3. RESULTS

Table 1 shows patient demographics for those who met our inclusion criteria. Age range was 41 years to 93 years, and 15 of the 29 were female. Table 2 tabulates the number of patients who were MVB-positive or -negative and the malignant brain tumor diagnoses.

For deep-seated metastatic brain tumors, majority (76.9%, 10 of 13) were MVB-positive while none of them presented with small medullary vein penetration. The three MVB-negative cases were classified so because extensive intratumoral dark signal in SWI made it impossible to discriminate if a small medullary vein was blocked outside or penetrated into the tumor. The sensitivity and specificity of the MVB sign for diagnosing deep-seated metastatic brain tumors were 76.9% and 100%, respectively, and diagnostic accuracy was 89.7%.

Neither of the two nonmetastatic tumor types exhibited MVBs. In all patients with PCNSL tumors and high-grade gliomas, there was at least one small medullary vein penetrating through tumors. The anatomical association between the small medullary veins and the tumors failed to differentiate between these two tumor types.

4. DISCUSSION

We identified a unique pattern of anatomical relationships between small medullary veins and tumors in SWI. The MVB

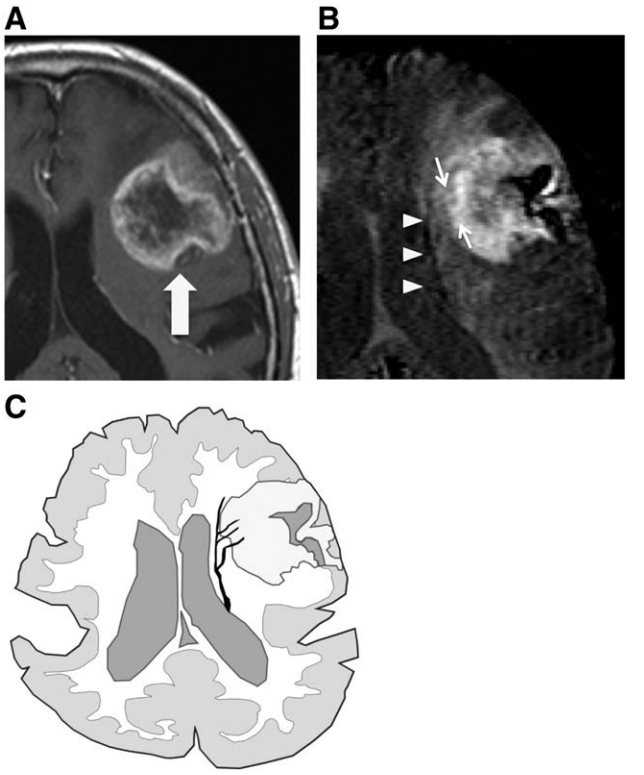

Fig. 4 Representative images of a subependymal vein near the tumor. A 74-year-old man diagnosed with high-grade glioma. A, Axial T1 post-contrast image showing the tumor (arrow) at the left frontal lobe. B, Axial susceptibility-weighted imaging (SWI) showing the subependymal vein (arrowheads) tangential to the tumor margin, and the small medullary vein (thin arrows) penetrating through the tumor. C, Sketch diagram illustrating the T1 postcontrast image (A) combined with the SWI (B) demonstrates the small medullary veins passing through the tumoral margin and converged to the subependymal vein between the tumoral margin and lateral ventricle.

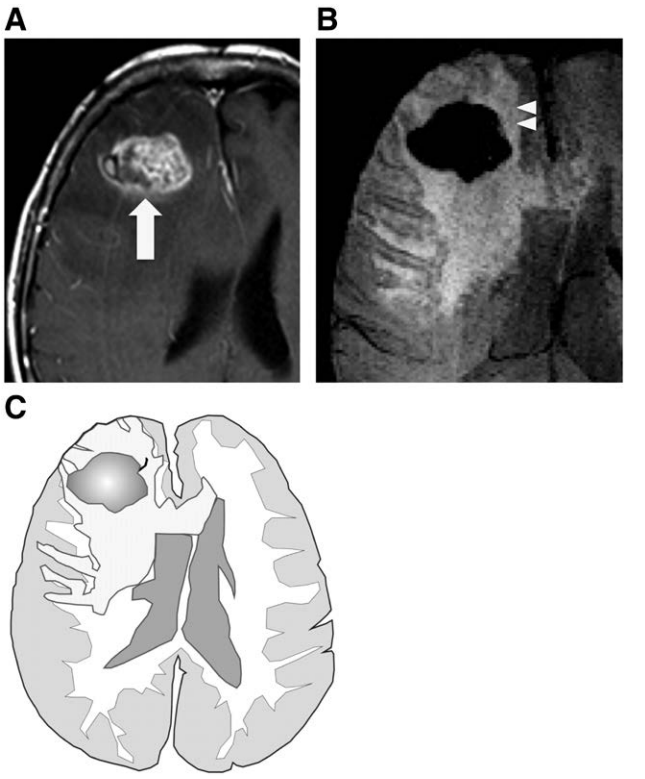

Fig. 5 Images of a medullary vein blockage (MVB) negative metastasis case. A 69-year-old woman diagnosed with metastatic squamous cell carcinoma. A, Axial T1 postcontrast image showing the tumor (arrow) at the right frontal lobe. B, Axial susceptibility-weighted imaging (SWI) showing extensively dark signal within the tumor and a small medullary vein (arrowheads) reaching the tumoral margin. C, Sketch diagram illustrating the T1 postcontrast image (A) combined with SWI (B). In this case, it is not possible to differentiate whether the vein continuously passed through tumor or stopped outside.

sign was common and exclusively present in deep-seated metastatic brain tumors. This is in accordance with the distinct growth patterns of metastatic tumors found in pathology. To the best of our knowledge, this is the first SWI study to apply the anatomical relationships between small medullary veins and tumors to differentiate deep-seated malignant brain tumors in adults.

It is well known that the borders between a metastatic tumor and the parenchyma are usually distinct without infiltration to the brain parenchyma.[17,18] Hence, most pre-existing vessels in brain parenchyma are likely to remain outside the tumor by either being destroyed or pushed away. This hypothesis was supported by our finding that MVB was detected by SWI in 10 of 13 patients in this study. Those patients who were classified as MVB-negative had extensive dark signal inside the tumor in SWI that prevent interpreter from differentiating if a small medullary vein was blocked outside or penetrated into the tumor (Fig. 5).

Interestingly, in two of the patients with metastatic tumors, there were also larger deep veins (anterior terminal vein and superior thalamostriate vein, respectively) mildly displaced by tumors. These deep veins are subependymal veins and run tangentially to tumoral margins. Both of them were close by the relatively large metastatic tumors (the diameter was 5.8 cm for one in the left frontal lobe and 4.7 cm for another in the right peri-trigonal region, while the mean diameter of the metastatic tumors was 4.0 cm). The mass effect and perifocal edema normally presented in large metastases might have displaced these large veins before destructing or blocking them.

Metastatic tumors of the brain are typically located in the corticomedullary junctions and usually do not require biopsy unless the tumor origin is unknown. In this study, biopsy-proven metastases represented difficult differential diagnoses. Atypical location for a metastatic brain tumor usually presents a challenging preoperation diagnosis, and the presence of the MVB

Table 1

Demographic data, patients with malignant brain tumors

	Number of patients	Female (%)	Mean age ± SD, years	Single lesion (%)	Tumor diameter ± SD, cm
PCNSL	11	5 (45%)	73.3 ± 5.8	4 (36%)	4.1 ± 1.7
High-grade glioma	5	2 (40%)	71.4 ± 10.7	4 (80%)	4.5 ± 1.2
Metastasis	13	8 (62%)	62.5 ± 12.7	7 (54%)	4.0 ± 1.3
Total	29	15 (52%)	66.6 ± 13.5	15 (52%)	4.1 ± 1.4

PCNSL = primary central nervous system lymphoma.

Table 2

The presence of MVB in three types of deep-seated malignant brain tumors

	MVB (+), n	MVB (–), n
PCNSL	0	11
High-grade glioma	0	5
Metastasis	10	3

MVB = medullary vein blockage; PCNSL = primary central nervous system lymphoma.

sign in the medullary vein territory can improve the diagnostic accuracy for deep-seated metastatic brain tumors.

Metastatic brain tumors are managed differently from those that are PCNSLs and high-grade gliomas. For example, a primary lesion will be sought out before biopsy if the cancer history is unknown. In this study, we found that MVB was seen exclusively in SWI for deep-seated metastatic brain tumors with a relative high accuracy of 89.7%. This finding assures that application of the MVB sign in clinical practice would likely be beneficial.

Histologically, a PCNSL typically demonstrates patchy, poorly demarcated, angiocentric proliferation of tumor cells that invade the parenchyma or subarachnoid space through the perivascular cuffs.[22] Lymphoma cells tend to infiltrate pre-existing parenchymal vessels rather than destruct them, and the tumor is usually deeply seated. Similarly, high-grade gliomas are among the most vascularized malignant tumors and show an infiltrative growth pattern. The malignant cells proliferate, and this is followed by endothelium proliferation and abundant angiogenesis.[23] Due to the growth patterns, these two tumor types tend to engulf small medullary veins within the tumor mass. Therefore, it is not surprising that in this study the two types of tumor presented no MVB, and commonly demonstrated continuous penetration of small medullary veins through the tumor. The high-grade gliomas may also show small medullary vein passing through the nonenhanced tumoral areas (Fig. 4) because mixed grades of high-grade gliomas were not unusual, and the microscopic infiltrative margin could not easily be delineated in postcontrast images.

Small medullary vein penetration in SWI could not be used to differentiate PCNSLs from high-grade gliomas given that this study included a small number of cases. However, it could well be a typical sign for PCNSL; it was detected in all 11 PCNSLs in this study, and similar results can be found in other locations throughout the human body. Examples include the "sandwich sign" of lymphomas involving the mesentery,[24] the CT "angiogram sign" of primary pulmonary lymphomas,[25] and the "small-vessel sign" of lymphomas involving peripheral lymph nodes.[26,27] Without the penetration sign, PCNSLs might need to be evaluated carefully. Further studies would be helpful for differentiating PCNSLs from other malignant brain tumors.

This study has limitations. This study recruited only pathology confirmed brain tumors; therefore, the population size is small. Only 29 tumors met our inclusion criteria, limiting the level of detailed analysis. For example, the numbers of GBM cases in the current study were too small (five patients) for statistical analysis. The relatively low occurrence of our research target—deep brain tumors that required a biopsy—explained partly why the case numbers are small. Nonetheless, those types of tumors are diagnostic challenges and our finding provides a neuroimaging feature that has not been described before. Additionally, this retrospective study lacked a one-to-one radiology-pathology correlation to demonstrate the image findings in the tissue sample. However, the entire picture of the relationship between medullary veins and the tumor, as detected by SWI, could be difficult to confirm pathologically through a regular small-sized tissue biopsy. Finally, SWI resolution in our protocol limited the comprehensive observation of the three-dimensional anatomical relationships between the tumors and medullary veins even after using reformatted coronal and sagittal views. This could be resolved in the future using faster and higher-resolution image acquisition, available from a 3-Tesla MR imaging machine.

In conclusion, the unique MVB sign delineating the anatomical relationship between medullary veins and deep-seated brain tumors provides an additional diagnostic clue about the brain metastasis in the medullary vein territory. This sign could be useful for preoperatively differentiating deep-seated metastatic tumors from the other two common primary malignant brain tumors.

ACKNOWLEDGMENTS

We thank Dr. Chia-Wei Li, Department of Radiology, Wan Fang Hospital, Taipei Medical University, for making the illustrating diagrams and Dr. Chin-Hsuan Lin, Wellcome Centre for Human Neuroimaging, Queen Square Institute of Neurology, University College London, for polishing English writing.

REFERENCES

1. Batchelor T, Loeffler JS. Primary CNS lymphoma. *J Clin Oncol* 2006;**24**:1281–8.
2. Giese A, Westphal M. Treatment of malignant glioma: a problem beyond the margins of resection. *J Cancer Res Clin Oncol* 2001;**127**:217–25.
3. Soffietti R, Rudā R, Mutani R. Management of brain metastases. *J Neurol* 2002;**249**:1357–69.
4. Al-Okaili RN, Krejza J, Woo JH, Wolf RL, O'Rourke DM, Judy KD, et al. Intraaxial brain masses: MR imaging-based diagnostic strategy–initial experience. *Radiology* 2007;**243**:539–50.
5. Cha S. Neuroimaging in neuro-oncology. *Neurotherapeutics* 2009;**6**:465–77.
6. Kono K, Inoue Y, Nakayama K, Shakudo M, Morino M, Ohata K, et al. The role of diffusion-weighted imaging in patients with brain tumors. *AJNR Am J Neuroradiol* 2001;**22**:1081–8.
7. Wang W, Hu Y, Lu P, Li Y, Chen Y, Tian M, et al. Evaluation of the diagnostic performance of magnetic resonance spectroscopy in brain tumors: a systematic review and meta-analysis. *PLoS One* 2014;**9**:e112577.
8. Haacke EM, Xu Y, Cheng YC, Reichenbach JR. Susceptibility weighted imaging (SWI). *Magn Reson Med* 2004;**52**:612–8.
9. Reichenbach JR, Haacke EM. High-resolution BOLD venographic imaging: a window into brain function. *NMR Biomed* 2001;**14**:453–67.
10. Reichenbach JR, Venkatesan R, Schillinger DJ, Kido DK, Haacke EM. Small vessels in the human brain: MR venography with deoxyhemoglobin as an intrinsic contrast agent. *Radiology* 1997;**204**:272–7.
11. Furtner J, Schöpf V, Preusser M, Asenbaum U, Woitek R, Wöhrer A, et al. Non-invasive assessment of intratumoral vascularity using arterial spin labeling: a comparison to susceptibility-weighted imaging for the differentiation of primary cerebral lymphoma and glioblastoma. *Eur J Radiol* 2014;**83**:806–10.
12. Radbruch A, Wiestler B, Kramp L, Lutz K, Bäumer P, Weiler M, et al. Differentiation of glioblastoma and primary CNS lymphomas using susceptibility weighted imaging. *Eur J Radiol* 2013;**82**:552–6.
13. Haddar D, Haacke E, Sehgal V, Delproposto Z, Salamon G, Seror O, et al. Susceptibility weighted imaging. Theory and applications. *J Radiol* 2004;**85**:1901–8.
14. Ogawa S, Lee TM, Kay AR, Tank DW. Brain magnetic resonance imaging with contrast dependent on blood oxygenation. *Proc Natl Acad Sci U S A* 1990;**87**:9868–72.
15. Egemen E, Solaroglu I. Anatomy of cerebral veins and dural sinuses. In: *Primer on cerebrovascular diseases*. Philadelphia, PA: Academic Press; 2017, p. 32–36.
16. Gerstner ER, Batchelor TT. Primary central nervous system lymphoma. *Arch Neurol* 2010;**67**:291–7.
17. Nathoo N, Chahlavi A, Barnett GH, Toms SA. Pathobiology of brain metastases. *J Clin Pathol* 2005;**58**:237–42.
18. Pekmezci M, Perry A. Neuropathology of brain metastases. *Surg Neurol Int* 2013;**4**(Suppl 4):S245–55.

19. Reichenbach JR, Jonetz-Mentzel L, Fitzek C, Haacke EM, Kido DK, Lee BC, et al. High-resolution blood oxygen-level dependent MR venography (HRBV): a new technique. *Neuroradiology* 2001;**43**:364–9.
20. Sampetrean O, Saga I, Nakanishi M, Sugihara E, Fukaya R, Onishi N, et al. Invasion precedes tumor mass formation in a malignant brain tumor model of genetically modified neural stem cells. *Neoplasia* 2011;**13**:784–91.
21. Ono M, Rhoton AL Jr, Peace D, Rodriguez RJ. Microsurgical anatomy of the deep venous system of the brain. *Neurosurgery* 1984;**15**:621–57.
22. Sugita Y, Muta H, Ohshima K, Morioka M, Tsukamoto Y, Takahashi H, et al. Primary central nervous system lymphomas and related diseases: pathological characteristics and discussion of the differential diagnosis. *Neuropathology* 2016;**36**:313–24.
23. Alves TR, Lima FR, Kahn SA, Lobo D, Dubois LG, Soletti R, et al. Glioblastoma cells: a heterogeneous and fatal tumor interacting with the parenchyma. *Life Sci* 2011;**89**:532–9.
24. Mueller PR, Ferrucci JT Jr, Harbin WP, Kirkpatrick RH, Simeone JF, Wittenberg J. Appearance of lymphomatous involvement of the mesentery by ultrasonography and body computed tomography: the "sandwich sign". *Radiology* 1980;**134**:467–73.
25. Vincent JM, Ng YY, Norton AJ, Armstrong P. CT "angiogram sign" in primary pulmonary lymphoma. *J Comput Assist Tomogr* 1992;**16**:829–31.
26. Majer MC, Hess CF, Kölbel G, Schmiedl U. Small arteries in peripheral lymph nodes: a specific US sign of lymphomatous involvement. *Radiology* 1988;**168**:241–3.
27. Sumi M, Van Cauteren M, Nakamura T. MR microimaging of benign and malignant nodes in the neck. *AJR Am J Roentgenol* 2006;**186**:749–57.